Surface Integral Equation Method for Scattering by DB Objects with Sharp Wedges

Johannes Markkanen, Pasi Ylä-Oijala, and Ari Sihvola

Department of Radio Science and Engineering
Aalto University School of Electrical Engineering
PO Box 13000, FI-00076 AALTO, Finland
johannes.markkanen@aalto.fi, pasi.yla-oijala@aalto.fi, ari.sihvola@aalto.fi

Abstract – A surface integral equation method is used to analyze time-harmonic electromagnetic scattering by arbitrarily shaped three-dimensional DB objects with sharp wedges. At the DB boundary surface, the electric and magnetic flux densities $\boldsymbol{D}$ and $\boldsymbol{B}$ normal to the surface are zero. The DB boundary conditions are enforced by expanding the unknown equivalent surface current densities with divergence-free loop basis functions. The equations are tested with Galerkin's method. The integral equation method is applied to investige field behavior at sharp DB wedges and the results are compared with the quasistatic solution in order to determine the accuracy of numerical solution at the sharp DB wedges.

Index Terms – DB boundary condition, field singularity, integral equation method.

I. INTRODUCTION

In computational electromagnetics, boundary conditions are often used as approximations of real material interfaces. The perfect electric conductor (PEC) boundary condition, which requires the vanishing of the tangential component of the electric field at the boundary surface, is probably the most well-known and commonly used boundary condition. It is often used as an approximation of conducting surfaces, for example metallic surfaces at low frequencies. There are also other boundary conditions that can be useful in computional electromagnetics. Especially since they can be used for modelling exotic material interfaces, e.g. PEMC [1]. In [2] the use of such canonical surfaces in computational electromagnetics have been summarized.

Electromagnetic soft surfaces [3], on which the power does not propagate along the surface, have many micro- and millimeterwave engineering applications. For example, they can be used for reducing coupling between radiating elements in antenna arrays or creating rotational symmetric radiation patterns for horn antennas [4]. Anisotropic soft surfaces are generally fabricated by corrugated structures, which are quite difficult to model by using standard numerical softwares, because they contain a lot of fine details. A relatively easy way to approximate isotropic soft surfaces is to apply a DB boundary condition [5] in calculations.

The DB boundary condition requires that the normal components of the electric and magnetic flux densities vanish at the boundary. Analytical solutions for objects involving the DB boundaries have been studied in [5, 6, 7], and the integral-equation-method based numerical solution for the scattering by DB objects was introduced in [8]. However, in most practial cases, a discretization of geometry leads to sharp wedges and corners which can cause problems for numerical calculations. At these sharp wedges and corners, fields can be singular. This fact gives motivation to analyze behavior of fields near DB wedges. It is possible to solve field behavior near sharp wedges by using quasistatic analysis, because the geometry is independent of any scale parameter, and therefore, the incident field can be analyzed by using static approach. A quasistatic solution is a well-known result for PEC and dielectric wedges [9, 10]. In this paper, we use a similar approach for analyzing field behavior near the DB wedge. Also, we compare the quasistatic solution with the integral-equation-method based nu-

merical solution, and study the accuracy of the solution at the DB wedge.

II. DB BOUNDARY CONDITION

The DB boundary condition, introduced in [5], requires that the normal components of the electric and magnetic flux densities $\boldsymbol{D}, \boldsymbol{B}$ vanish on the surface:

$$\boldsymbol{n} \cdot \boldsymbol{D} = 0, \quad \boldsymbol{n} \cdot \boldsymbol{B} = 0. \tag{1}$$

In linear, homogeneous, and isotropic medium, where permittivity ϵ and permeability μ are constants, the DB boundary condition (1) can be expressed as

$$\boldsymbol{n} \cdot \boldsymbol{E} = 0, \quad \boldsymbol{n} \cdot \boldsymbol{H} = 0. \tag{2}$$

A look at the Poynting vector illuminates the character of a DB boundary. The average propagating power-density can be calculated from the real part of the complex Poynting vector

$$< S(t) >= \frac{1}{2} \Re\{\boldsymbol{E} \times \boldsymbol{H}^*\}, \tag{3}$$

where $\boldsymbol{H}^*$ denotes the complex conjugate of the magnetic field $\boldsymbol{H}$. At the DB boundary, the following can be written:

$$\boldsymbol{n} \times (\boldsymbol{E} \times \boldsymbol{H}^*) = \boldsymbol{E}(\boldsymbol{n} \cdot \boldsymbol{H})^* - (\boldsymbol{n} \cdot \boldsymbol{E})\boldsymbol{H}^* = 0. \tag{4}$$

Hence, the Poynting vector at the DB boundary has only the normal component and the tangential component vanishes. A soft surface has been defined [3] as a surface where the power flux along the boundary is zero. Therefore, the DB boundary is an isotropic soft surface.

III. INTEGRAL EQUATIONS FOR DB BOUNDARY

Consider an arbitrarily shaped three-dimensional object with the DB boundary condition in a homogeneous background medium and an incident time harmonic field ($e^{-i\omega t}$). The surface of the object is denoted by S and the electromagnetic parameters of the background medium are ε and μ. Our goal is to solve scattering of the electromagnetic waves by this obstacle. We begin with the following representation of the total time-harmonic electric and magnetic fields [11]

$$\begin{aligned} \Omega \boldsymbol{E} &= -\nabla \mathcal{S}(\boldsymbol{E}_n) + i\omega\mu \mathcal{S}(\boldsymbol{J}) - \mathcal{K}(\boldsymbol{M}) + \boldsymbol{E}^p \\ \Omega \boldsymbol{H} &= -\nabla \mathcal{S}(\boldsymbol{H}_n) + i\omega\varepsilon \mathcal{S}(\boldsymbol{M}) + \mathcal{K}(\boldsymbol{J}) + \boldsymbol{H}^p, \end{aligned} \tag{5}$$

where Ω is the relative solid angle subtended by the surface ($\Omega = 1/2$ on smooth surfaces), $\boldsymbol{E}_n$ and $\boldsymbol{H}_n$ are the normal components of the fields at the surface, $\boldsymbol{J} = \boldsymbol{n} \times \boldsymbol{H}$ and $\boldsymbol{M} = -\boldsymbol{n} \times \boldsymbol{E}$ are the equivalent electric and magnetic surface current densities, respectively, $\boldsymbol{E}^p$ and $\boldsymbol{H}^p$ are the primary fields, and $\boldsymbol{n}$ is the outer unit normal vector of the surface. The surface integral operators are defined as

$$\mathcal{K}(\boldsymbol{F})(\boldsymbol{r}) = \nabla \times \mathcal{S}(\boldsymbol{F})(\boldsymbol{r}), \tag{6}$$

$$\mathcal{S}(\boldsymbol{F})(\boldsymbol{r}) = \int_S G(\boldsymbol{r}, \boldsymbol{r}') \boldsymbol{F}(\boldsymbol{r}') \, \mathrm{d}S(\boldsymbol{r}), \tag{7}$$

where G is the free space Green's function

$$G(\boldsymbol{r}, \boldsymbol{r}') = \frac{e^{ik|\boldsymbol{r}-\boldsymbol{r}'|}}{4\pi|\boldsymbol{r}-\boldsymbol{r}'|}, \tag{8}$$

$\boldsymbol{r}$ is the observation point, $\boldsymbol{r}'$ is the source point, and $k = \omega\sqrt{\varepsilon\mu}$ is the wavenumber of the background. Let us define two surface integral operators as

$$\begin{aligned} \mathcal{F}_t &= -\boldsymbol{n} \times \boldsymbol{n} \times \mathcal{F} \\ \mathcal{F}_r &= \boldsymbol{n} \times \mathcal{F}. \end{aligned} \tag{9}$$

Due to the DB boundary conditions (2), $\boldsymbol{E}_n$ and $\boldsymbol{H}_n$ can be removed from (5). Normalizing the fields in the following way (to get better balance between the unknowns and the matrix elements, [12])

$$\tilde{\boldsymbol{E}} = \sqrt{\varepsilon}\boldsymbol{E}, \quad \tilde{\boldsymbol{H}} = \sqrt{\mu}\boldsymbol{H}, \tag{10}$$

so called T- equations is obtained by taking the tangential components

$$\begin{bmatrix} \tilde{\boldsymbol{H}}_t^p \\ \tilde{\boldsymbol{E}}_t^p \end{bmatrix} = \begin{bmatrix} -ik\mathcal{S}_t & -\frac{1}{2}\mathcal{I}_r - \mathcal{K}_t \\ \frac{1}{2}\mathcal{I}_r + \mathcal{K}_t & -ik\mathcal{S}_t \end{bmatrix} \begin{bmatrix} \tilde{\boldsymbol{M}} \\ \tilde{\boldsymbol{J}} \end{bmatrix}. \tag{11}$$

Another set of equations, called N- equations, is obtained by taking the cross product with the normal vector $\boldsymbol{n}$

$$\begin{bmatrix} -\tilde{\boldsymbol{E}}_r^p \\ \tilde{\boldsymbol{H}}_r^p \end{bmatrix} = \begin{bmatrix} \frac{1}{2}\mathcal{I}_t - \mathcal{K}_r & ik\mathcal{S}_r \\ -ik\mathcal{S}_r & \frac{1}{2}\mathcal{I}_t - \mathcal{K}_r \end{bmatrix} \begin{bmatrix} \tilde{\boldsymbol{M}} \\ \tilde{\boldsymbol{J}} \end{bmatrix}. \tag{12}$$

The integral equation formulations for DB objects contaning only T- or N- equations, however, suffer from internal resonances, i.e., the solution is not unique at certain frequencies. Internal resonances can be eliminated by combining equations (11) and (12) in

a similar fashion as the T- and N- equations are combined in [13] in the case of penetrable objects. This gives the following combined field integral equation (CFIE) formulation for DB objects

$$\begin{bmatrix} -\tilde{\boldsymbol{F}}_r \\ \tilde{\boldsymbol{F}}_t \end{bmatrix} = \begin{bmatrix} \mathcal{N}_t & -\mathcal{N}_r \\ \mathcal{N}_r & \mathcal{N}_t \end{bmatrix} \begin{bmatrix} \tilde{\boldsymbol{M}} \\ \tilde{\boldsymbol{J}} \end{bmatrix}, \tag{13}$$

with

$$\mathcal{N}_t = \frac{1}{2}\mathcal{I}_t - \mathcal{K}_r - ik\mathcal{S}_t \text{ and } \tilde{\boldsymbol{F}}_t = \tilde{\boldsymbol{H}}_r^p + \tilde{\boldsymbol{E}}_t^p. \tag{14}$$

IV. NUMERICAL SOLUTION TO THE INTEGRAL EQUATIONS

Integral equations (11–13) are solved numerically with the method of moments [14]. First, the unknown equivalent electric $\boldsymbol{J}$ and magnetic $\boldsymbol{M}$ surface current densities are represented as linear combinations of known tangential vector basis functions $\boldsymbol{f}$ and $\boldsymbol{g}$

$$\begin{aligned} \boldsymbol{J} &\approx \sum_{k=1}^{N} j_k \boldsymbol{f}_k \\ \boldsymbol{M} &\approx \sum_{l=1}^{M} m_l \boldsymbol{g}_l, \end{aligned} \tag{15}$$

where j_k and m_l are scalar coefficients. By using Maxwell's equations and certain vector identities, we can find a relation between the normal components of the fields and the divergences of the equivalent surface currents

$$\begin{aligned} \nabla_s \cdot \boldsymbol{J} &= i\omega\varepsilon \boldsymbol{n} \cdot \boldsymbol{E} \\ \nabla_s \cdot \boldsymbol{M} &= i\omega\mu \boldsymbol{n} \cdot \boldsymbol{H}. \end{aligned} \tag{16}$$

As we can see, on the surface of a DB object the surface divergences of the currents vanish (if $\omega \neq 0$) due to the DB boundary conditions (2). Therefore, we have to expand both the electric and magnetic equivalent surface current with a set of basis functions which span a solenoidal vector space. We have used the RWG loop basis functions [15] to expand the equivalent currents, and the equations are tested with Galerkin's scheme using the RWG loop functions as testing functions.

A numerical solution requires calculation of singular integrals because the Green's function becomes singular when the distance between the source point and the observation point goes to zero. These integrals are evaluated by using the singular subtraction technique [16].

V. FIELD BEHAVIOR AT A DB WEDGE

Singularities of the fields appear near sharp wedges and corners with a proper incident field, and these singularities can cause problems for the numerical solution. For example, in case of a PEC or dielectric wedge the fields are singular, and hence, we need to use mesh refinement near the wedges and corners in order to obtain an accurate solution. In this section, we study singularities of fields in the case of a DB wedge.

Consider a three-dimensional sharp wedge with a DB boundary condition. Since the wedge is sharp, we can use quasistatic approximation. Therefore, the electric field $\boldsymbol{E}$ near the wedge can be expressed in terms of the electrostatic potential $\boldsymbol{E} = -\nabla\phi$. In the static and source-current free case we can also express the magnetic field in terms of a scalar potential $\boldsymbol{H} = -\nabla\phi_m$, but here we only consider the electric field because the analysis is identical in both cases.

We know that the potential function outside the wedge must satisfy the Laplace's equation

$$\nabla^2\phi = 0, \tag{17}$$

because the divergence of the electric field must be zero in a source free region. Also, the field must satisfy the boundary condition at the surface. We can approximate this problem with the two-dimensional infinite wedge, see Fig. 1.

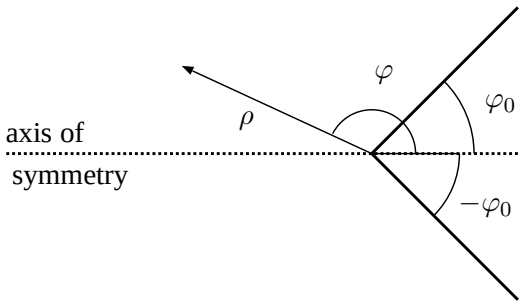

Fig. 1. Two-dimensional infinite wedge. Surface of the wedge is at $\varphi = \varphi_0$ and $\varphi = -\varphi_0$.

In the polar coordinate system the Laplace's equation (17) can be expressed as

$$\nabla^2\phi(\rho,\varphi) = \frac{1}{\rho}\frac{\partial}{\partial\rho}\left(\rho\frac{\partial\phi(\rho,\varphi)}{\partial\rho}\right) + \frac{1}{\rho^2}\frac{\partial^2\phi(\rho,\varphi)}{\partial\varphi^2} = 0, \tag{18}$$

where ρ is the radial coordinate and φ is the angular coordinate. This equation can be solved by the separation of variables

$$\phi(\rho,\varphi)=\sum_n P_n(\rho)\Phi_n(\varphi), \tag{19}$$

which leads to two separate differential equations

$$\frac{\partial^2\Phi_n(\varphi)}{\partial\varphi^2}+\nu_n^2\Phi_n(\varphi)=0 \tag{20}$$

$$\rho\frac{\partial}{\partial\rho}\left(\rho\frac{P_n(\rho)}{\partial\rho}\right)-\nu_n^2P_n(\rho)=0. \tag{21}$$

General solutions for the equations (20) and (21) are

$$\begin{aligned}\Phi_n(\varphi)&=A_n\sin(\nu_n\varphi)+B_n\cos(\nu_n\varphi)\\ P_n(\rho)&=C_n\rho^{\nu_n}+D_n\rho^{-\nu_n},\end{aligned} \tag{22}$$

where A_n, B_n, C_n, and D_n are the unknown coefficients. The coefficient D_n must be zero, because a negative exponent $\rho^{-\nu_n}$ leads to an infinite energy at the origin.

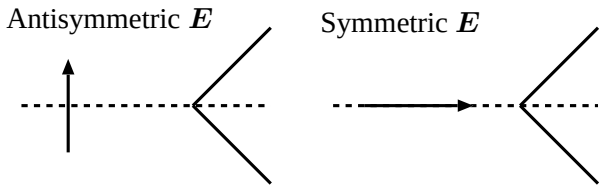

Fig. 2. Antisymmetric and symmetric excitations with respect to the wedge.

If the incident field is symmetric with respect to the plane of symmetry $\varphi=0$ (see Fig. 2), the potential function can be expressed as

$$\phi(\rho,\varphi)=\sum_n B_n\rho^{\nu_n}\cos(\nu_n(\pi-\varphi)), \tag{23}$$

if $\varphi_0\le\varphi\le 2\pi-\varphi_0$. By taking the gradient of the potential function, we obtain the electric field

$$\begin{aligned}\boldsymbol{E}(\rho,\varphi)&=-\nabla\phi(\rho,\varphi)\\ &=-\boldsymbol{u}_\rho\sum_n B_n\rho^{\nu_n-1}\nu_n\cos(\nu_n(\pi-\varphi))\\ &\quad-\boldsymbol{u}_\varphi\sum_n B_n\rho^{\nu_n-1}\nu_n\sin(\nu_n(\pi-\varphi)).\end{aligned} \tag{24}$$

By using the DB boundary condition $\boldsymbol{u}_\varphi\cdot\boldsymbol{E}=0$ at $\varphi=\varphi_0$, we find that

$$\sum_n B_n\rho^{\nu_n-1}\nu_n\sin(\nu_n(\pi-\varphi_0))=0, \tag{25}$$

which is satisfied if

$$\nu_n=\frac{\pi}{\pi-\varphi_0}n,\quad n=1,2,... \tag{26}$$

Next, we consider the antisymmetric case where the incident field is normal to the plane of symmetry ($\varphi=0$). Now the potential function is

$$\phi(\rho,\varphi)=\sum_n A_n\rho^{\nu_n}\nu_n\sin(\nu_n(\pi-\varphi)), \tag{27}$$

if $\varphi_0\le\varphi\le 2\pi-\varphi_0$, and the electric field can be expressed as

$$\begin{aligned}\boldsymbol{E}(\rho,\varphi)&=-\nabla\phi(\rho,\varphi)\\ &=-\boldsymbol{u}_\rho\sum_n A_n\rho^{\nu_n-1}\nu_n\sin(\nu_n(\pi-\varphi))\\ &\quad+\boldsymbol{u}_\varphi\sum_n A_n\rho^{\nu_n-1}\nu_n\cos(\nu_n(\pi-\varphi)).\end{aligned} \tag{28}$$

In the case of the DB boundary condition

$$\sum_n A_n\rho^{\nu_n-1}\nu_n\cos(\nu_n(\pi-\varphi_0))=0, \tag{29}$$

which is satified if

$$\nu_n=\frac{\pi}{2(\pi-\varphi_0)}n,\quad n=1,3,5,... \tag{30}$$

Parameter ν_n defines the order of singularity of field, since the field strength is related to a term ρ^{ν_n-1}. It is easy to see that the field has a singularity if the smallest value of the parameter $\nu_n<1$. Figure 3 shows the value of the parameter ν_1 as a function of angle φ_0. We can see that the DB wedge has a singularity if the excitation field is antisymmetric, and the angle $\varphi_0<90$ degrees.

It is important to note that a solution in the case of an arbitrarily polarized field can be found as a linear combination of symmetric and antisymmetric excitations. This analysis is valid also if $\boldsymbol{E}$ is replaced by $\boldsymbol{H}$ because of the symmetry of the DB boundary condition.

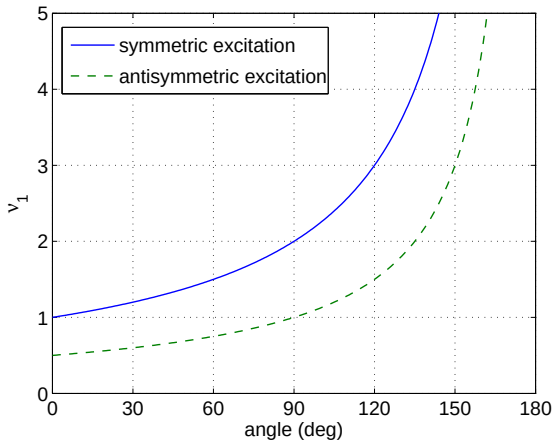

Fig. 3. Parameter ν_1 as a function of angle φ_0 with either symmetric or antisymmetric excitations. The field is singular if the parameter $\nu_1 < 1$.

VI. NUMERICAL RESULTS

Let us first investigate the behavior of the equivalent surface currents near a 90° wedge, which is characterized by either DB or PEC boundary conditions. We can solve the problem for the DB boundary in the static case by using equations (26) and (30) and requiring $\varphi_0 = \pi/4$. In Table 1, we see singularity factors ($\rho^{\nu_n - 1}$) in case of 90° DB and PEC wedges with symmetric and antisymmetric excitations. The PEC case can be solved in a similar way as the DB case, but we have to apply the PEC boundary conditions $\boldsymbol{u}_\rho \cdot \boldsymbol{E} = 0$ and $\boldsymbol{u}_\varphi \cdot \boldsymbol{H} = 0$.

Table 1: Singularities of 90° DB and PEC wedges

Excitation	Field	DB	PEC
Symmetric $\boldsymbol{E}^i$	$\boldsymbol{E} \cdot \boldsymbol{u}_\rho$	$\rho^{\frac{1}{3}}$	0
Symmetric $\boldsymbol{H}^i$	$\boldsymbol{H} \cdot \boldsymbol{u}_\rho$	$\rho^{\frac{1}{3}}$	$\rho^{\frac{1}{3}}$
Symmetric $\boldsymbol{E}^i$	$\boldsymbol{E} \cdot \boldsymbol{u}_\varphi$	0	$\rho^{-\frac{1}{3}}$
Symmetric $\boldsymbol{H}^i$	$\boldsymbol{H} \cdot \boldsymbol{u}_\varphi$	0	0
Antisymmetric $\boldsymbol{E}^i$	$\boldsymbol{E} \cdot \boldsymbol{u}_\rho$	$\rho^{-\frac{1}{3}}$	0
Antisymmetric $\boldsymbol{H}^i$	$\boldsymbol{H} \cdot \boldsymbol{u}_\rho$	$\rho^{-\frac{1}{3}}$	$\rho^{-\frac{1}{3}}$
Antisymmetric $\boldsymbol{E}^i$	$\boldsymbol{E} \cdot \boldsymbol{u}_\varphi$	0	$\rho^{\frac{1}{3}}$
Antisymmetric $\boldsymbol{H}^i$	$\boldsymbol{H} \cdot \boldsymbol{u}_\varphi$	0	0

We can see that the tangential components of both fields are singular in the case of the DB wedge with antisymmetric excitation, but with symmetric excitation fields are not singular. Also, we can see that the normal components of fields vanish at the wedge due to the DB boundary condition. In case of the PEC wedge, the tangential electric field and the normal component of the magnetic field are zero. With the symmetric electric field incident, the normal component of the electric field is singular but the tangential component is non-singular. Also, the antisymmetric magnetic field incident creates a singularity to the tangential component of the magnetic field at the wedge.

Now, we know how fields behave near DB wedges, and we can study the accuracy of the surface-integral-equation-method based solution near DB wedges. Consider a small cube with DB boundary condition. This cube with edge length a is illuminated by a linearly polarized planewave with wavelength $\lambda = 10\,a$. We can choose the alignment of the cube so that the behavior of fields at the wedge corresponds to the 2-D case with either symmetric or antisymmetric excitations.

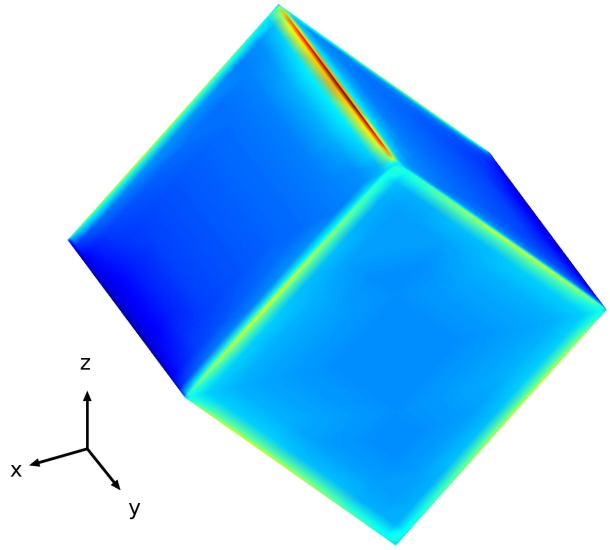

Fig. 4. Real part of the equivalent electric surface current density at the surface of DB cube. The cube is illuminated by a planewave which is propagating along z-axis and the electric field is polarized along y-axis and the magnetic field along x-axis. The equivalent current $\boldsymbol{J}$ has a singularity at the top edge, because the incident magnetic field is antisymmetric with respect to the wedge on top.

Figure 4 shows the real part of the equivalent electric surface current density $\boldsymbol{J}$ on the surface of the DB cube. We can see that the equivalent electric surface current ($\boldsymbol{J} = \boldsymbol{n} \times \boldsymbol{H}$) is singular at the wedge on top, because in this case we have an antisymmetric incident magnetic field with respect to the wedge on top.

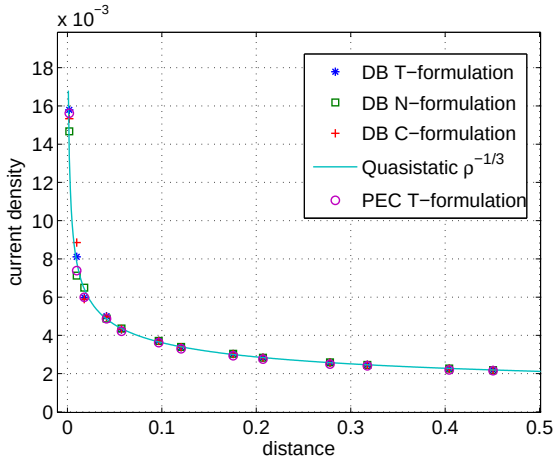

Fig. 5. Amplitude of the equivalent electric surface current density as a function of distance from the sharp 90 degree DB and PEC wedges. Solutions are obtained by using different formulations of surface integral equation method and quasistatic analysis.

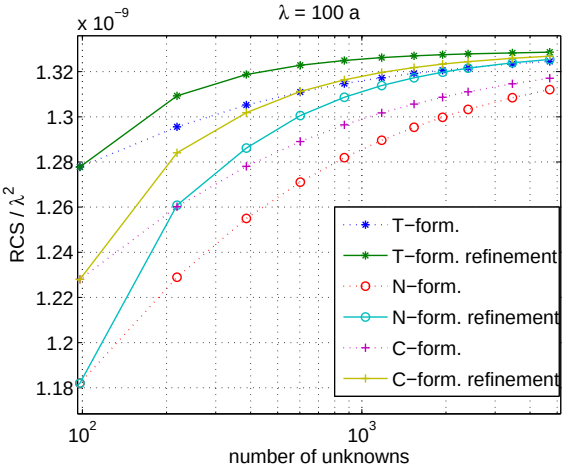

Fig. 6. Calculated backscattered radar cross section of a cube with edge length a and wavelength $\lambda = 100\,a$ as a function of number of unknowns. T-, N- and C- formulations have been applied. The cube is discretized by using triangular meshes with or without mesh refinement on the edges. Solid lines correspond to the cases with mesh refinements and dotted lines without mesh refinements.

In Figure 5, the amplitude of the equivalent electric surface current density is shown as a function of distance from the wedge. The calculations are done by using T-, N-, and C- formulations and the results are compared with the quasistatic solution.

As can be seen, all three formulations give almost identical results for the equivalent current densities near 90° DB wedge, and the numerical results have a good agreement with the quasistatic solution. However, there are some variations in the amplitude of currents between formulations especially if the distance to the sharp wedge is short. Figure 5 also shows the behavior of the equivalent surface current at the PEC wedge. The PEC case is calculated by using the conventional tangential electric field integral equation (EFIE) formulation with RWG basis and testing functions [17].

As the quasistatic analysis predicts, at the DB and PEC wedge tangential fields have the same order of singularity and the numerical results agree with it. It is important to note that the normal component of the electric field is singular in case of the PEC wedge, if the incident electric field is symmetric with respect to the wedge. We know that there is a relation between the normal component of field and the divergence of the equivalent surface current (16), but this singularity does not affect the result in Figure 5 because the incident electric field is not symmetric at the wedge.

Let us next study the convergence of the numerical solution in case of a DB cube. The setup is the same as in Figure 4. In Figure 6, the backscattered radar cross section (RCS) as a function of the number of unknowns is shown. The edge length of the cube is a and the wavelength is $\lambda = 100\,a$. In Figure 7 we can see the convergence of RCS with wavelength $\lambda = 2\,a$. We have used T-, N-, and C-formulations for calculations, and the surface of the cube is discretized by triangular mesh with mesh refinement on the edges, or without mesh refinement on the edges.

In this example wavelengths are 100 and 2 times the edge length of the cube, and hence, both frequencies are not at internal resonant frequencies. This means that the solutions of T-, N-, and C- formulations are unique. We can see that the T- formulation gives the most accurate results for backscatted RCS. The convergence of N- formulation is quite slow. The accuracy of C- formulation is between T- and N- formulations which makes sense because C- formulation is a combination of T- and N- formulations. This agrees with the earlier results in the PEC case [18] where T-formulation agrees with EFIE, N-formulation with MFIE, and C-formulation with CFIE, respectively. Figures 6 and 7 also show that the solutions converge faster if mesh refinements on wedges are used.

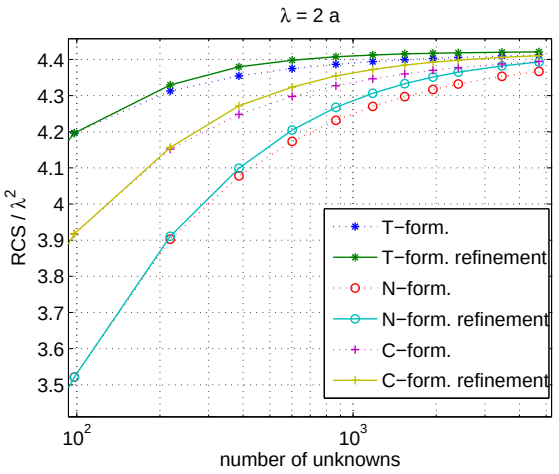

Fig. 7. Calculated backscattered radar cross section of a DB cube with wavelength $\lambda = 2\,a$. Otherwise the setup is the same as in Figure 6.

VII. CONCLUSIONS

In this paper, the accuracy of a surface-integral-equation based solution for DB objects has been studied. A quasistatic solution for the field near DB wedges has been derived and the results have been compared with numerical calculations. The numerical examples demonstrate that the surface-integral-equation-method based solution is quite accurate near DB wedges even if the field is singular at the wedge. We have also showed that the tangential magnetic field at the PEC wedge has the same order of singularity as that of the DB wedge. The normal component of the electric field can be singular at the PEC wedge, but there is not such singularity at the DB wedge, because normal components of fields vanish at the DB boundary. However, the effect of this singularity to the equivalent surface current in the case of the PEC wedge is much weaker than the effect of the singularity in the tangential field. Therefore, we need to use similar mesh refinements at the DB wedges as the PEC wedges in order to obtain an accurate solution.

ACKNOWLEDGMENT

This study was supported by the Academy of Finland projects 125979 and 124204.

REFERENCES

[1] A. Sihvola, P. Ylä-Oijala, and I. Lindell, "Scattering by PEMC (Perfect Electromagnetic Conductor) Spheres using Surface Integral Equation Approach," *ACES Journal*, vol. 22, no. 2, pp. 236–249, 2007.

[2] P. R. Kildal, A. Kishk, and Z. Sipus, "Introduction to Canonical Surfaces in Electromagnetic Computations: PEC, PMC, PEC/PMC Strip Grid, DB Surface," *26th Annual Review of Progress in Applied Computational Electromagnetics, Tampere, Finland, 2010*, pp. 514–519.

[3] P.-S. Kildal, "Definition of Artificially Soft and Hard Surfaces for Electromagnetic Waves," *Electronics Letters*, vol. 24, pp. 168–170, Feb. 1988.

[4] P.-S. Kildal, "Artificially Soft and Hard Surfaces in Electromagnetics," *IEEE Trans. Antennas and Propagation*, vol. 38, pp. 1537 –1544, Oct. 1990.

[5] I. V. Lindell and A. H. Sihvola, "Electromagnetic Boundary and Its Realization with Anisotropic Metamaterial," *Physical Review E (Statistical, Nonlinear, and Soft Matter Physics)*, vol. 79, no. 2, p. 026604, 2009.

[6] I. V. Lindell and A. H. Sihvola, "Spherical Resonator with DB-Boundary Conditions," *Progress In Electromagnetics Research Letters*, vol. 6, pp. 131–137, 2009.

[7] A. Sihvola, H. Wallén, P. Ylä-Oijala, M. Taskinen, H. Kettunen, and I. V. Lindell, "Scattering by DB Spheres," *Antennas and Wireless Propagation Letters, IEEE*, vol. 8, pp. 542–545, 2009.

[8] J. Markkanen, P. Ylä-Oijala, and A. Sihvola, "Computation of Scattering by DB Objects with Surface Integral Equation Method," *IEEE Trans. Antennas and Propagation*, vol. 59, pp. 154 –161, Jan. 2011.

[9] J. G. Van Bladel, *Electromagnetic Fields*. Wiley Interscience, 2nd ed., 2007.

[10] J. D. Jackson, *Classical Electrodynamics*. John Wiley & Sons, 3rd ed., 1998.

[11] J. A. Stratton, *Electromagnetic Theory*. McGraw-Hill Company, New York, London, 1941.

[12] M. Taskinen and P. Ylä-Oijala, "Current and Charge Integral Equation Formulation," *IEEE Trans. Antennas and Propagation*, vol. 54, pp. 58–67, Jan. 2006.

[13] P. Ylä-Oijala and M. Taskinen, "Application of Combined Field Integral Equation for Electromagnetic Scattering by Dielectric and Composite Objects," *IEEE Trans. Antennas and Propagation*, vol. 53, pp. 1168 – 1173, Mar. 2005.

[14] R. F. Harrington, *Field Computation by Moment Methods*. IEEE press, New York, 1993.

[15] G. Vecchi, "Loop-Star Decomposition of Basis Functions in the Discretization of the EFIE," *IEEE Trans. Antennas and Propagation*, vol. 47, pp. 339 –346, Feb. 1999.

[16] S. Järvenpää, M. Taskinen, and P. Ylä-Oijala, "Singularity Subtraction Technique for High-Order Polynomial Vector Basis Functions on Planar Triangles," *IEEE Trans. Antennas and Propagation*, vol. 54, pp. 42 – 49, Jan. 2006.

[17] S. Rao, D. Wilton, and A. Glisson, "Electromagnetic Scattering by Surfaces of Arbitrary Shape," *IEEE*

Trans. Antennas and Propagation, vol. 30, pp. 409–418, May 1982.

[18] P. Ylä-Oijala, M. Taskinen, and S. Järvenpää, "Analysis of Surface Integral Equations in Electromagnetic Scattering and Radiation Problems," *Engineering Analysis with Boundary Elements*, vol. 32, pp. 196–209, 2008.

Johannes Markkanen was born in Kerava, Finland, in 1984. He received the M.Sc. (Tech.) degree in Electrical Engineering from the Helsinki University of Technology (TKK), Espoo, Finland, in 2009. Currently, he is working toward the D.Sc. (Tech.) degree in the Aalto University, School of Electrical Engineering, Department of Radio Science and Engineering, Finland. His research interests include integral equation methods in computational electromagnetics.

Pasi Ylä-Oijala received the M.Sc. and Ph.D. degrees in Applied Mathematics from the University of Helsinki, Helsinki, Finland, in 1992 and 1999, respectively. Currently, he is working as a senior researcher with the Aalto University, School of Electrical Engineering, Department of Radio Science and Engineering, Finland. His field of interest focuses on the development of efficient and stable integral equation based formulations and algorithms in computational electromagnetics, and analysis of electromagnetic phenomena.

Ari Sihvola was born in 1957 in Valkeala, Finland. He received the degrees of Diploma Engineer in 1981, Licentiate of Technology in 1984, and Doctor of Technology in 1987, all in Electrical Engineering, from the Helsinki University of Technology (TKK), Finland. Besides working for TKK and the Academy of Finland, he was visiting engineer in the Research Laboratory of Electronics of the Massachusetts Institute of Technology, Cambridge, in 1985-1986, and in 1990-1991, he worked as a visiting scientist at the Pennsylvania State University, State College. In 1996, he was visiting scientist at the Lund University, Sweden, and for the academic year 2000-01, he was visiting professor at the Electromagnetics and Acoustics Laboratory of the Swiss Federal Institute of Technology, Lausanne. In the Summer of 2008, he was visiting professor at the University of Paris XI, France. Ari Sihvola is professor of electromagnetics in Aalto University School of Electrical Engineering (former name before 2010: Helsinki University of Technology) with interest in electromagnetic theory, complex media, materials modelling, remote sensing, and radar applications. He is Chairman of the Finnish National Committee of URSI (International Union of Radio Science), official member for Finland of URSI Commission B (Fields and Waves), and Fellow of IEEE. He was awarded the five-year Finnish Academy Professor position starting August 2005. He is also director of the Finnish Graduate School of Electronics, Telecommunications, and Automation (GETA).